ACADEMIA ROMÂNĂ
Revue Roumaine de Chimie
http://web.icf.ro/rrch/

Rev. Roum. Chim
2018, *63(2)*, 133-142

STRUCTURAL CHARACTERIZATION AND ANTIBACTERIAL ACTIVITY OF PP/HDPE/CLAY/TiO_2 NANOCOMPOSITES PREPARED BY REACTIVE EXTRUSION

Hicham KOUADRI,[a,b*] Ferhat DJERBOUA[a] and Ouahiba BOURICHE[a,b]

[a] Department of Process Engineering, University of Ferhat Abbas Setif-1 19000, Algeria
[b] The Center of Scientific and Technical Research in Physicochemical Analyses (CRAPC), BP 384, Zone Industrially Bou_Ismail RP 42004 Tipaza Algeria

Received June 12, 2017

Blends of polypropylene (PP) and high-density polyethylene (HDPE) were prepared by reactive blending in the presence of dicumyl peroxide (DCP) as a free radical generator, maleic anhydride (MAH) as a cross-linking agent and organo-montmorillonite (O-Mt) as filler. Titanium dioxide (TiO_2) was added as a anti UV agent known as well for its antimicrobial activity. This formulation was aimed to see how an incompatible blend will behave in the presence of the above cited ingredients and if it will have an anti-bacterial activity. The compounding of the ingredients was carried out in internal brabender mixer. The resulting materials were characterized using different techniques: dynamical rheological analysis (DRA), differential scanning calorimetry (DSC), fourier transform infrared spectroscopy (FTIR), atomic force microscopy (AFM), and mechanical testing. The results showed that the presence of titanium dioxide in the blends PP/HDPE leads to the destruction of the octahedral and tetrahedral structure of the clay (exfoliation form), results confirmed by FTIR analysis where it has been observed that the peaks associated with the octahedral structure have disappeared. AFM showed a smooth surface for the materials mainly those with high relatively organo-montmorillonite content and TiO_2 which showed improvement in their mechanical properties. Antibacterial efficiency of the composites depends on the dispersion and the concentration of the TiO_2 particles and it was concluded that composites with either low or high content of TiO_2 showed antibacterial property.

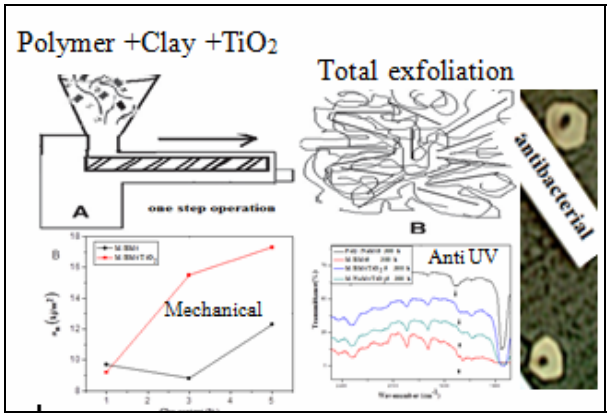

INTRODUCTION

After their first appearance in 1988[1] Polymer/clay nanocomposites constitute a relatively large field of research. Recently, the use of nanoclays has opened a new route in polymer blends where it is found that clays enhance the compatibility in this type of systems[2–4]. This has attracted considerable attention in both scientific and industrial fields, because a very small amount of clay can significantly improve the properties of the polymer. Clays like phyllosilicates, such as montmorillonite, have been used as reinforcing materials for polymers owing to their high aspect ratio (length/diameter). This characteristic confers unique intercalation/exfoliation characteristics to the polymer/ clay nanocomposites, which govern the enhancement of some interesting polymer properties.[5]

Attention was given to the blends of polypropylene (PP) with high-density polyethylene (HDPE), as with most thermoplastics, these polymers are immiscible and need to be made compatible. As a

*Corresponding author: chinpolyhim@yahoo.fr

compatibilizer for this system, maleic anhydride (MAH) was found to be a very efficient agent.[6] In addition, when compared PP/HDPE/MAH blends with their corresponding low clay content composites, these later materials showed improved properties, mainly, their strength, their heat resistance and their impact resistance.[7]

It is well established that some inorganic particles when introduced in a polymeric matrix not only increase the mechanical strength of the polymers but can also provide antibacterial property and ultraviolet resistance. However, there are very few studies on the antibacterial properties of such polymer composites. This has been well reviewed with polymeric materials which contain ZnO.[8] Such products made from plastics can be sterilized by ethylene oxide or ionizing radiation. But, they can still be contaminated or infected by microorganisms when being exposed to air. There are some methods to make polymers antibacterial and melt mixing with an antibacterial agent is the most convenient method.[9] TiO_2 is one of these agents. We can recall that TiO_2 is a semiconductor photocatalyst that can generate hydroxyl radicals (OH) under UV light. This is very important in catalysis reactions and antibacterial properties of TiO_2.[10]

Concerning the preparation of polymer or polymer blend/layered silicate nanocomposite, this can be achieved through three ways; solution, *in situ* polymerization and melt blending. Solution and *in situ* polymerization routes are commonly used, but these are expensive processes. Melt blending is an economically favorable process and by far is the most used process.[11]

The main objective of this work is to evaluate the effect of organo clay of the type montmorillonite (O-Mt) and its content on the structure and the mechanical properties of the PP/HDPE blends. The (TiO_2) was added in order to increase the ultraviolet resistance and to bring the antimicrobial activity. The composites were prepared by melt compounding in the presence of dicumyl peroxide (DCP) as a free radical generator and maleic anhydride (MAH) as a cross-linking agent. In relation to the composition of different formulation, a correlation between the morphology, the mechanical properties, the UV resistance and the antibacterial activity was made.

EXPERIMENTAL

1. Materials

The following materials were used in this investigation:

Polypropylene (PP) Sabic-500P, Melt Flow index at 230°C and 2.16 kg; 3g/10 min. D 1238 density at 23°C 905kg/m3 D 792.

Polyethylene (HDPE)Sabic-F00952, Melt flow index at 190 °C and 2.16 kg; 0.05g/10 min ISO 1133, density 23°C 952 kg/m³ISO 118.

Dicumyl peroxide (DCP) which was supplied by Bayer ltd. It has a density of 1 g/cm^3 with a decomposition temperature of 130 °C.

Maleic anhydride (MAH) purchased from (sigma-Aldrich).

Benzyl tributyl ammonium chloride ($C_{19}H_{34}NCl$), (Flukapurum>98% (Cl)).

The unmodified clay (Mt called maghnite) was supplied by ENOF (Algeria). The cation exchange capacity (CEC) is about 1.15×10^{-2}mol/g.

Titanium dioxide (TiO_2) rutile 99.9, powder, (sigma-Aldrich).

Lamp UV 32wat (λ 300-400 nm) distance at 20 cm.

2. Organophilic clay preparation

The raw bentonite was first crushed and then sieved. Then, 30 g were dispersed in a 1l aqueous sodium chloride (NaCl) solution (1N), and the mixture was stirred for 24 h. The aqueous supernatant phase was replaced four times with the above cited solution. The final suspension was washed with distilled water five times, until the chloride ions have completely disappeared. Then, the suspension was left for 48 h to be decanted. After sedimentation, the suspension was centrifuged, and the wet powder was dried. The solid was grounded in mortar. The obtained powder (5 g) was dispersed in a hot aqueous solution (80°C) containing (10^{-2} M) of benzyl tributyl ammonium chloride ($C_{19}H_{34}NCl$), and the mixture was stirred for 3 h. To eliminate the organic cations, the obtained suspension was washed 5 times with a 50/50 water/ethanol solution at 60°C. The organophilic montmorillonite thus obtained was dried for 36 h before it was crushed, sieved and stored [7].

3. Compounding of the ingredients

Before blending, the polymers in granules forms with the weight composition (50/50) were dry-mixed physically in a plastic bag. The mixing and the compounding of the polymers and the additives (DCP, MAH, O-Mt and TiO_2) were carried out in a one step in a Brabender Haake Rheocord (Cergy-Pontoise, France) with 50 mL chamber volume, at 180°C and 60rpm, and where the torque-time rheograms were recorded for each formulation.

The resulting materials were compression molded into 1mm thin films on a Zwick machine (Ulm, Germany), model 7102, working at a pressure of 150 kg/cm^2). The compression was performed at 180^{0}C for 10min cycle with 4min for preheating and 2 min degassing and 4 mn for pressing. The following formulations were prepared; the amount of each ingredient is expressed in PHR (parts per hundred resin) (Table 1).

Table 1

List of samples and their abbreviations

Sample	PP	/HDPE	MAH	NaMt	O-Mt	TiO_2
M	50	/50	1	-	-	-
Poly NaMt1	50	/50	-	1	-	-
Poly NaMt3	50	/50	-	3	-	-
Poly NaMt5	50	/50	-	5	-	-
M/BMt1	50	/50	1	-	1	-
M/BMt3	50	/50	1	-	3	-
M/BMt5	50	/50	1	-	5	-
M/BMt/TiO_2 1	50	/50	1	-	1	1
M/BMt/TiO_2 3	50	/50	1	-	3	3
M/BMt/TiO_2 5	50	/50	1	-	5	5

4. Characterization technics

4. 1. Dynamical rheological analysis (DRA)

The properties of the melt mixing and the compounding during the preparation phase of the different formulations were studied considering their dynamic rheological analysis. For this a Brabender-type plastograph was used. The study of the torque variation as a function of time during the mixing reports the rheological behavior of different reactive compounds. This approach is used to assess the contribution either chemical or physical of each component of the formulation. The rotors speed was chosen so that the viscosity change of the melt can be detected, and which may be associated to cross-linking reaction in the polymer phases and/or the lubricating action of the reaming ingredients.

4.2. Fourier transform infrared spectroscopy (FTIR)

The FTIR spectrophotometry is a well-known technique in detecting chemical changes which may occur during the blending and the compounding of polymers and formulation ingredients. In the present study, the FTIR spectra were obtained for **M, PolyNaMt, M/BMt, M/BMt/TiO_2**. The analyses were carried out on Shimadzu IRAFFINITY-1S apparatus and the different samples in the form of thin films (200 um) obtained by compression molding were considered. The analyses were performed in the wavenumber range (450-4 400 cm^{-1}).

4.3 Differential scanning calorimetry (DSC)

The calorimetry study was performed on Mettle Toledo Star System 30 equipment. Sample weight was around 15 mg. The samples were heated in nitrogen atmosphere from 25 up to 200 °C at a heating rate of 10°C/min. The method was used in order to determine the fusion enthalpies (ΔHm) and the melting temperatures (Tm) of the polymers making the blend. The degree of crystallinity was calculated using the theoretical melting enthalpy values for 100 % crystalline polymers: for 100 % crystalline PE, ΔHm = 293.86 J/g and for 100 % crystalline PP, ΔHm = 207.33 J/g.[12]

4.4 Atomic Force Microscopy (AFM)

Atomic force microscopy is a powerful characterization tool in polymer science, capable of revealing surface structures with a superior spatial resolution.[13] The universal character of repulsive forces between the tip and the sample, which are employed for surface analysis in AFM, enables examination of even single polymer molecules without disturbance of their integrity.[14] Being initially developed as the analogue of scanning tunneling microscopy (STM) for the high-resolution profiling of non-conducting surfaces, AFM has been developed into a multifunctional technique suitable for characterization of topography, adhesion, mechanical, and other properties on scales from tens of microns to nanometers.[15] The AFM surface analysis in this study was realized on films using an Asylum Research MFP-3D STAND ALONE equipment.

5. Mechanical properties

5.1. Impact testing

The impact strength tests were conducted at room temperature on Resil Impactor machine "IMPACTOR CEAST"). Each test was repeated at five times in order to ensure the good reproducibility of measurements. The izod impact resistance of both unnotched specimens of all samples was determined.

5.2. Tensile testing

The Young's modulus, the tensile strength at the yield point and at break as well as the elongation at break of every material were obtained from stress-strain measurements performed on a Zwick/RoellProline tensile machine. The specimen dimensions: width 10mm, thickness 1 mm. The grip length was 88 mm. The Crosshead speed was 5 mm/min, and an average of three test values was taken.

6. Antibacterial test

This test was used to demonstrate the possible antibacterial activity of our samples. This test is inspired from the ISO 20645 originally developed to determine the antibacterial activity of a sample by measuring a zone of inhibition of bacterial growth. Around this zone we notice the diffusion of the antibacterial agent out of the sample provided that it is soluble in water of the culture medium.

RESULTS AND DISCUSSION

Dynamical rheological analysis of blends (DRA)

The analysis of the torque-time evolution during the melt mixing exhibited by the binary blend based on PP/HDPE (50/50) matrix in the presence of dicumyl peroxide (DCP) as a free radical

generator and maleic anhydride (MAH) as a cross-linking agent, reveals complex crosslinking reactions involving the different components (Fig. 1). It illustrates the different steps of the torque-time evolution for the system. From this figure, it can be seen that initially, the polymers melts and the torque decreases to a minimum value, which describes the transformation from the solid to the molten state (point T_A). As the crosslinking reaction begins, the torque increases until it reaches the maximum value (point T_B). After which, a partial decrease of the torque is observed. This slight decrease is attributed to the partial destruction of the network already formed. Then a leveling of the torque takes place with an almost constant torque value at the point T_c, usually higher than T_A. A similar power curve was obtained with the ternary blend composed of PP/LDPE/EPDM treated with the same system.[16] The power curve characteristics depend strongly on the temperature used for the mixing (Fig. 2), where it can be noticed that the low temperature (150 ^{0}C) was appropriate for a high cross-linking density in the reacting phase. Further treatment will lead to the destruction of the network and a leveling of the stationary torque at a value not far from those obtained at higher temperatures.

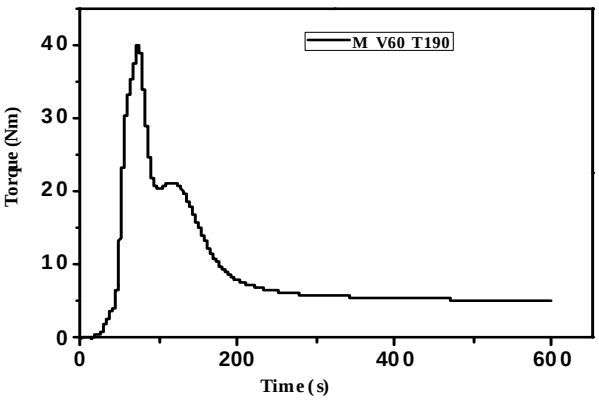

Fig. 1 – Variation of the torque *versus* time for PP/HDPE/MAH at (60 rpm and 190°C).

The experimental results of the torque-time evolution at 170 and 190 °C for the PP/HDPE blends how that the torque decreases with time, being even lower in the presence of peroxide (Figure 2). This is due to the attack by the peroxide radicals (particularly at the tertiary carbons of PP, which are the more reactive sites), to form macroradicals by disproportionation or by cyclization of the end groups, this is attributed mainly to the fact that PP degradation, in the presence of peroxide, results in shorter chains through scission reactions. This means that the viscosity will diminish, owing to the decrease in the molecular weight. Such a result has been already reported by Braun *et al*. on polypropylene with peroxide 10. In this study we have changed the temperature to reduce the degradation of PP and promote cross-linking with HDPE at 160 and 150°C, where an increase in the torque values was observed. This was an indication that crosslinking reactions occurred, originating a molecular weight increase (Figure 2).

Concerning the effect of the presence of the additives (Mt,TiO_2) on the mixing characteristics of the compounds, can be illustrated in figure 3 which represents the torque-time evolution at 180°C for the composites PP/HDPE/MAH/Mt, and TiO_2 with a peroxide content of 1 % wt. The evaluation of T_B and T_C at the equilibrium shows that the crosslinking effect starts to be apparent from (M/BMt3). This positive deviation is proportional to the degree of crosslinking in the matrix. As mentioned previously, the formation of a complex network takes place, and the evolution of the torque is affected by the PP degradation. However, the presence of TiO_2 has no apparent effect on the torque-time evolution.

Infrared spectroscopy analysis (FTIR)

Figures 4 and 5 show the FTIR spectra of untreated raw clay, M/BMt, M/BMt/TiO_2 and Poly/NaMt/TiO_2. From the results shown in Figure 4 and Table 2, it was observed that the peaks associated with the tetrahedral structure of the clay remain in the final structure of the M/BMt/TiO_2 samples, while the peaks associated with the octahedral structure disappear; this is also observed in the case of Poly/NaMt/TiO_2. Thus, the type of reactions which took place during the compounding led to structure changes particularly in the presence of TiO_2 where nearly the main peaks related to Mt have disappeared. It is rather difficult to show it but the destruction of the octahedral structure could support the consequence of this assumption. The reaction mechanism is complex, but the results suggest that the presence of TiO_2 active groups in the system may be involved in the destruction of the octahedral and tetrahedral structure of the clay. In addition, there are also variations in the peak intensities related PP/HDPE/BMt/TiO_2 and PP/HDPE/NaMt/TiO_2 matrices, for both pure and nanoblend mixtures.[15]

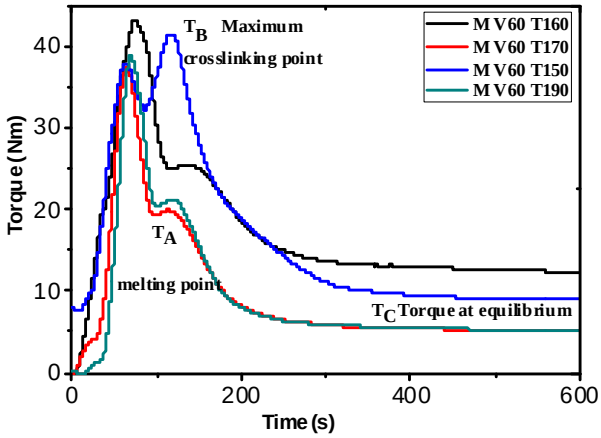

Fig. 2 – Variation of the torque *versus* time for (PP/HDPE/MAH) at different temperatures.

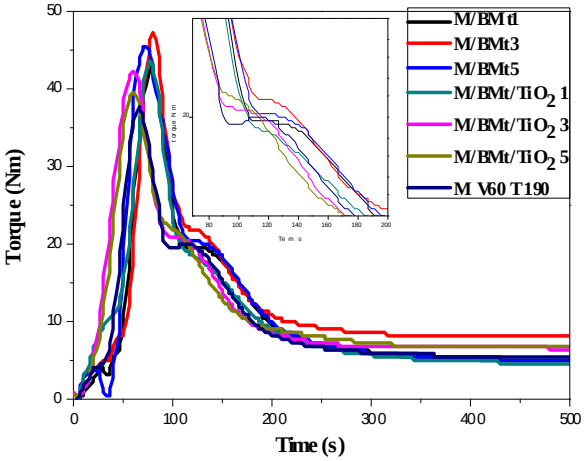

Fig. 3 – Variation of the torque *versus* time for (M, M/BMt 1, 3, 5 M/BMt /TiO_2 1, 3, 5) at 180 °C.

Table 2

Important Fourier transform infrared spectroscopy (FTIR) bands of raw clay M/BMt/TiO_2, Poly/NaMt/ TiO_2

Bands assignment	Position in raw clay (cm^{-1})	M/BMt/TiO_2	Poly/NaMt/TiO_2
Si-O-Si deformation	466	Disappeared	Low
Al-O-Si deformation	522	Disappeared	Low
Coupled Al-O and Si-O out of plane	628	Disappeared	Disappeared
Si-O Si-O stretching in quartz and silica	669 719	Low	Disappeared
	731	Low	Disappeared
Al Mg OH deformation	759	Disappeared	Disappeared
Al-Al-OH deformation		Disappeared	Disappeared

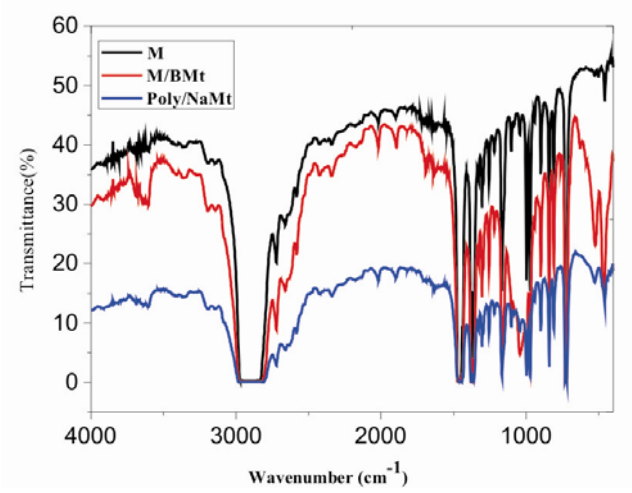

Fig. 4 – Variation of IR transmittance (%) of M, M/BMt and Poly/ NaMt.

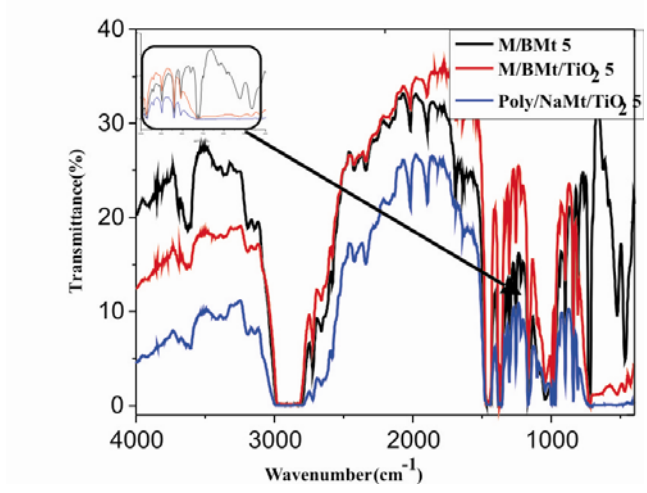

Fig. 5 – Variation of IR transmittance of M/BMt, M/BMt/TiO_2 5 and Poly/NaMt/TiO_2 5.

Table 3

Melting temperatures and melting enthalpies /for different blends based on PP/HDPE

Sample	ΔH_m : HDPE J/g	ΔH_m : PP J/g	T_m : HDPE °C	T_m : PP °C	Xc : HDPE %	Xc : PP %
M 160	10.71	5.65	134	165	26.36	27.18
M 180	9.50	3.11	137	167	26.77	28.45
poly/NaMt1	32.22	8.13	137	167	19.04	25.94
poly/NaMt5	43.19	13.57	139	169	15.30	23.22
M/BMt1	11.65	2.29	135	165	26.04	28.86
M/BMt5	2.30	1.92	132	159	29.22	29.04
M/BMt/TiO_2 1/160	23.30	12.30	135	165	22.07	23.85
M/BMt/TiO_2 1/180	23.47	7.71	138	168	22.01	26.15
M/BMt/TiO_2 5/160	3.59	2.92	136	166	28.78	28.54
M/BMt/TiO_2 5/180	3.20	1.91	133	163	19.13	29.04

Differential scanning calorimetry analysis (DSC)

The melting enthalpy (ΔH_m) and the melting temperature (T_m) of each of the polymer components, and their total degree of crystallinity were obtained and are reported in Table 3 for the different formulations. The results show that the values of T_m of HDPE and that of PP are not strongly affected and they are similar to those of the pure polymers and in some cases the difference does not exceed 4 °C.

From Table 3, it can be seen that the enthalpy of fusion of the polymers for the different formulations is strongly affected by the composition and is lower when compared to those of the two homopolymers. The samples Poly/NaMt1 and Poly/NaMt5 have the highest value. This indicates that the crystallization processes taking place in the polymers in the formulation are hundred. In addition, according to the T_m values, it can be said that there is an effect on the mode of crystallization of each crystalline part. This is due to the fact that when PP starts to crystallize, HDPE is still in the molten state, and this will affect the nucleation rate of the PP. On the other hand, when HDPE starts to crystallize, the PP is in a solid state and this will then affect the growing rate of HDPE crystallization. Therefore, we end up with smaller spherules 16. As a result, the crystallization modes of the two polymers are related to the chain dispersion and the crosslinking effect. In addition to that, the organophilic montmorillonite and the TiO_2 improve the close contact in the interphase confined space, resulting in a decrease of the crystallinity.

The effects of the organophilisation of the clay, the presence of TiO_2 and the temperature on the crystallisation properties of the polymer components making the matrices can be seen through the DSC curves (Figure 6). From the thermograms in (a) it can be concluded that when the clay is treated by the alkylammonium, the crystallization of the polymers is strongly hundred. This may be associated to the fact that the organophilisation led to the exfoliation of the clay. Concerning the presence of TiO_2 (b) in the formulation seems to enhance the development of crystallinity in both homopolymers with apparent increases in their melting points. This can be associated to the nucleating effect of TiO_2. On the other hand the temperature of mixing does affect the melting points as well as the degree of crystallinity in the polymers (c). It can be seen that the lower temperature favors the development of crystallinity with reduction in melting points values.

Atomic Force Microscopy (AFM)

AFM images were obtained on both blend of polymer and their nanocomposites at 5% inorganic clay and TiO_2 loading and these are shown in Figure 7: a, b, c, d. One can clearly see the presence of some clay tactoids as well some regions where the nano-dispersion is excellent. The quality of the nano-dispersion appears to be higher in the polymer TiO_2 system than in the polymer clay system. In the images at higher magnification, one can see both intercalated and delaminated regions. These systems should probably be described as mixed immiscible/intercalated/delaminated systems with surface roughness indices (RMS) respectively (32.51, 35.72, 35.95, and 23.68 nm), values which are in agreement with the FTIR and mechanical results.

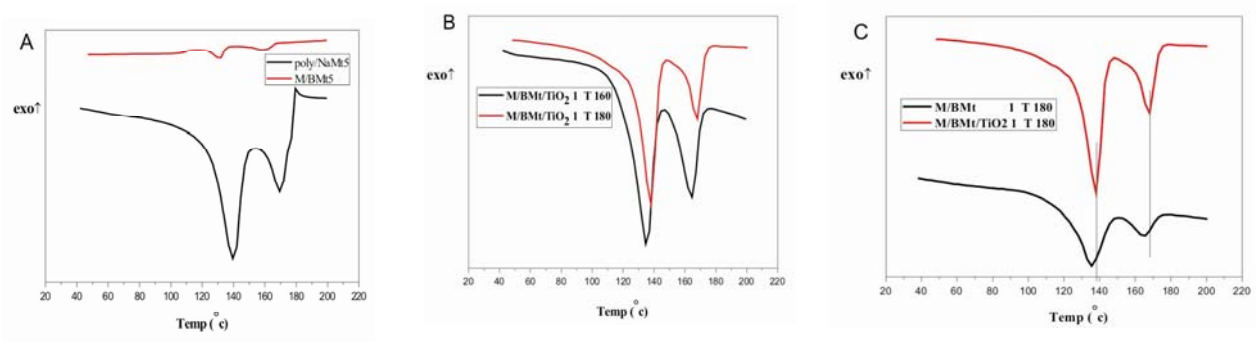

Fig. 6 – DSC curves of the different reactive blends based on (PP/HDPE):
a) effect of organophilisation, b) effect of TiO2 and c) effect of temperature of mixing.

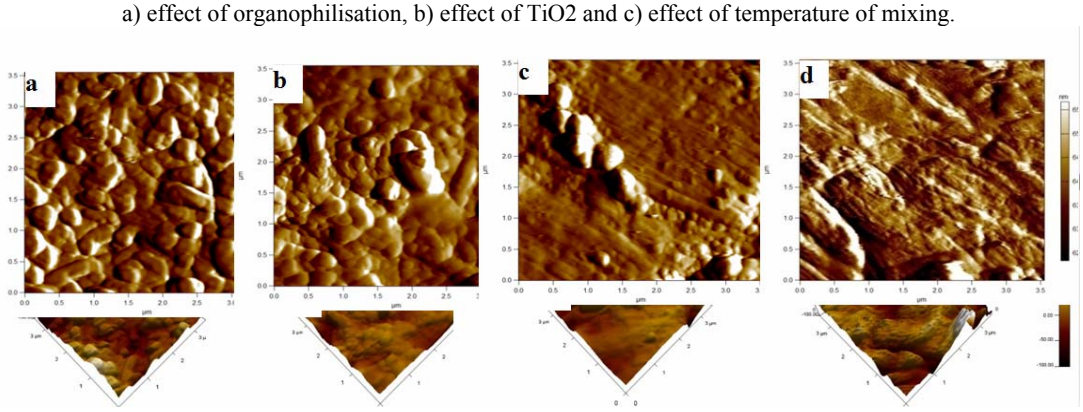

Fig. 7 – AFM topographic images of: a) M, b) Poly/NaMt, c) M/BMt, d) M/BMt/TiO_2.

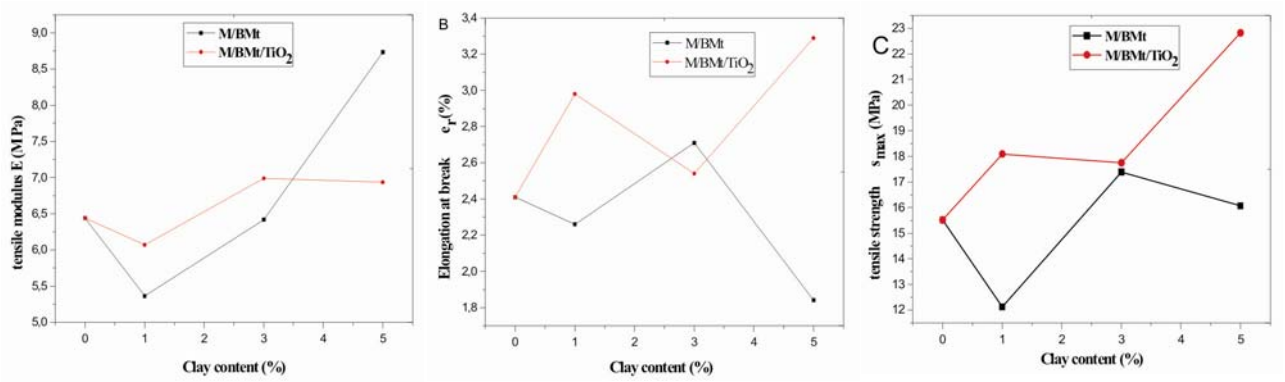

Fig. 8 – Mechanical properties of the materials:
(a) tensile modulus, (b) elongation at break, (c) tensile strength.

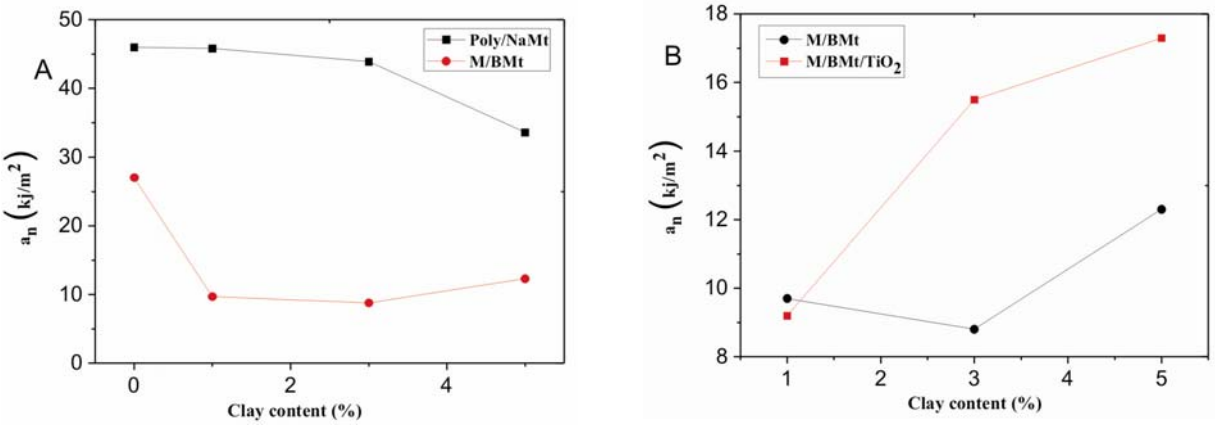

Fig. 9 – Impact strength for Poly/NaMt, M/BMt and M/BMt/TiO_2.

Tensile properties

The Young's modulus, the tensile stress, and the elongation at break are reported in figure 8 (a, b, c) for all the compositions. From these results, it can be inferred that the incorporation of clay in different weight percentages in PP/HDPE has not significantly affected its tensile properties.

Thus, only the Young's modulus slightly increases with the clay content in the range 1 to 5 wt. %. The sample with 5 wt. % clay shows the highest values for the tensile strength, and elongation at break. In addition, most of blends with clay present yield stress values similar to that of pure PP/HDPE/MAH. The results presented in figure 8 (a, b, c) show that the new materials are more rigid than PP/HDPE bends. This is attributed to the interaction between the polymer chains and the nanolayers clay. The presence of TiO2 increases all the cited mechanical parameters.

Impact strength

The impact sensitivity refers to the tendency of the material to break or crack on impact when the material is affected by a crack, fissure, or break. A high sensitivity denotes ductility, while a low sensitivity denotes pliability brittleness of the material. Figure 9 shows the impact sensitivity for the different formulation *versus* the clay loading. The impact sensitivity values decrease with the clay content, the uncompatibilized blend presents the highest impact strength, which means that, although the material is quite rigid and it presents a brittle behavior. As observed in figure 8 (c) where it is noticed that the presence of TiO_2 in the formulation enhances the strength of the material, similar remark can be made on the effect of TiO_2 on the impact strength.

Ultraviolet Resistance of TiO_2 in the composites Materials

In order to improve the ultraviolet resistance of the Polymeric mixture, materials containing TiO_2 have widely been investigated. However, it is found that introduction of a great number of inorganic particles accelerates the rate of photo-oxidative degradation of the polymer. For the montmorillonite (Mt) based nanocomposites, Qin *et al.*[17] and Morlat *et al.*[18] observed the detrimental influence of Mt particles on the photo-degradation rate of the PP matrix. However, addition of TiO_2 as filler cannot only increase the physical and mechanical properties, but also improves the ultraviolet resistance properties of polymer materials. This is due to the superior UV light screening effects offered by the TiO_2 particles incorporated into the materials.

The extent of photo-degradation of the different formulations was followed through the change in chemical structure due to the oxidation in the polymeric phases. This was done by monitoring their infrared spectra before and after an UV exposure for 300 h.

In figure 10 (a) are presented the infrared spectra of the different formulations. These show an increase in the intensity of the peak corresponding to carbonyl groups (1780 cm^{-1}) with the Mt content which proves that the clay induces the photo oxidation of the polymer. This result agrees with those mentioned previously.[17,18] On the contrary the presence of TiO_2 in the formulation seems to act in the opposite way to that of the clay.

In figure 10 (b) are presented the infrared spectra of the formulations varying in TiO_2 content. It is very clear that the peak of carbonyl diminishes when raising the quantity of TiO_2.

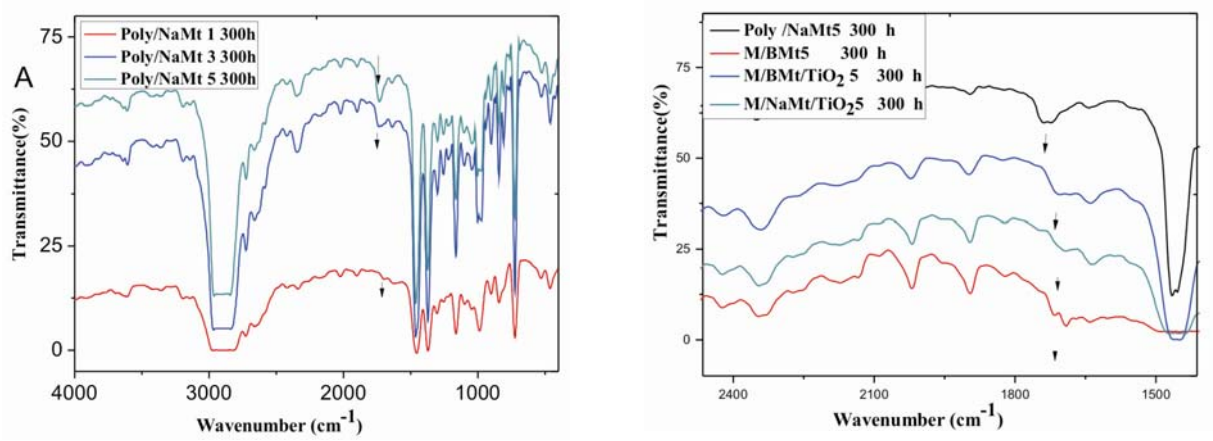

Fig. 10 – FTIR spectra for UV-irradiated; a: (poly/NaMt 1, 3, 5), b: (Poly/NaMt 5), (M/BMt 5) and (M/BMt/TiO_2 5).

A B C

Fig. 11. – Photographs of survival bacteria colonies obtained after 24 h incubation at 37 °C of a: (M/BMt), b : (M/BMt/TiO_2), c : (poly/NaMt/TiO_2).

Antibacterial activity of the materials

Polymers are widely used to prepare packing materials which demand high sanitary standard. They are also used in film production which offers all the conditions in a single material for the agriculture to solve the problems with greenhouses for farmers. Therefore materials with good mechanical properties, anti UV resistance and antibacterial activity are looked for. Such materials can find applications in hospitals spaces mainly operating rooms, laboratories and health equipment.

This has made polymer composites containing TiO_2 a subject of growing interest in science as well as in industry. TiO_2 is regarded as one of the most popular antimicrobial agents due to its high efficiency, nontoxicity, biocompatibility, low cost and a wide spectrum for preventing bacteria from growing and reproduction.

The antibacterial activity of the materials was determined by measuring a zone of inhibition of bacterial growth. Around this zone we notice the diffusion of the antibacterial agent out of the sample provided that it is soluble in water of the culture medium.

The micrographs in figure 11 show petri dishes containing culture medium and a :(M/BMt), b :(M/BMt/TiO_2), c :(poly/NaMt/TiO_2). From these it can be seen that the antibacterial effect is present in the formulation (b) where the clay is organophilic and its FTIR and AFM results indicated a state of exfoliation and excellent nano-dispersion. According to Linsebigler *et al.*,[19] smaller semiconductor particles increased the surface area, catalytic effect and therefore nano-sized particles have better antibacterial activity than micron-sized particles. M. Li *et al.*[8] reported that the antibacterial ability of ZnO-supported zeolite particle filled iPP composites is significantly higher than that of iPP filled by 10 wt% ZnO. It is attributed to the effect of the formed nano-sized ZnO on the surface of zeolite particles. Therefore, we suggested that ZnO-supported zeolites can provide an effective filler to increase antibacterial ability of ZnO and decrease the ZnO content for preparing antibacterial PP composites.

In this study, the composites with low and high TiO_2 content (M/BMt/$TiO_2$1 and M/BMt/TiO_2 5) have an antibacterial effect with a small zone of inhibition (Figure: 11 b). The absence of a wide distribution represented a very important result for two reasons ; it would cause low toxicity and would ensure antibacterial activity over time.[20] Only sodic clay/TiO_2 particles tended to agglomerate and bigger particles were observed in the matrix (Figure 7 b), a reason for the absence of the antibacterial effect (Figure 11 c).

CONCLUSIONS

Nanocomposite blends at different clay loadings were prepared by the mixture of the polymers with the Benzyl tributyl ammonium chloride modified clay. The DRA results show that binary blends based on PP/HDPE, as deduced from the torque time curves, present cross-linking reactions. This takes place in the molten state after polymer fusion. The intensity of the crosslinking depends on the used temperature and is the highest at 150°C. The mechanical results show an enhancement in the Young's moduli, which were obtained from the tensile testing. The addition of TiO_2 to the nanocomposites leads to the destruction of the octahedral and tetrahedral structure of the clay (exfoliation form); these results were confirmed by FTIR analysis where it has been observed that the peaks associated with the octahedral structure have disappeared. AFM indicated smooth surface for the materials mainly those with high relatively organo-

montmorillonite content and TiO_2 which showed improvement in their mechanical properties. A slight increase in crystallinity was observed with the increase in the clay content which could be explained by the possible nucleating effect of the clay nanoparticles.TiO_2 is a multifunctional material which cannot only improve mechanical properties, but also grant polymer materials with ultraviolet resistance and antimicrobial properties. The ultraviolet resistance and antimicrobial properties of TiO_2 in the composite blend materials have been studied. Although the addition of TiO_2 can increase the ultraviolet resistance of polymers, it is found that clay particles can accelerate the rate of photo-oxidation degradation of matrices. The antimicrobial properties were seen in the formulations where TiO_2 is present, the clay is organophilic and its FTIR and AFM results indicated a state of exfoliation and excellent nano-dispersion.

REFERENCES

1. A. Okada, Y. Fukushima, M. Kawasumi, S. Inagaki, A. Usuki, S. Sugiyama, T. Kuraunch and O. Kamigaito. (United States), Pat. 4,739,007, **1988**.
2. R. Jarrar, A. Mahmood and Y. Haik, *J. Appl. Polym. Sci*., **2012**, *124*, 1880–1890.
3. G. Wu and A. Cuculo, *Polymer*, **1999**, *40*, 1011–1018.
4. K. Jaehyun, K. Whanki, Y. Jusun and K. Ho-Jong, *Polymer(Korea)*, **2011**, *35*, 249–253.
5. K. Pramoda, M. Ashiq, I. Phang and L. Tianxi, *Polym Int*., **2005**, *54*, 226–232.
6. F. Chiu, H. Yen and C. Chen, *Polymer Testing*., **2010**, *29*, 706–716.
7. B. Samia, R. Doufnoune, H. Abdelhak and H. Nacceredine, C. Esperanza, *J. Polym. Eng.*, **2013**, *33*, 589–598.
8. L. Mei, L. Gu, J. Juan, Z. Zishou, D. Xin and M. Kancheng, *J. Mater. Sci. Technol*., **2015**, *31*, 331–339.
9. W. Zhaobo, L. Guicun, P. Hongrui and Z. Zhikun, *J. Mater. Sci*., **2005**, *40*, 6433–6438.
10. A. Mirigul and Y. Huseyin, *J. Mater. Sci. Technol*., **2012**, *28*, 686–692.
11. B. Fatma-Zohra, R. Lixia, B. Djafer, C. Esperanza, P. Marc, Z. Foued, B. Said, J. Francisco and C. Balta, *J. Polym. Eng*., **2014,** *35*, 181–190.
12. W. Bernhard and G. Janusz, "Advances in Polymer Science", vol. 60/61, Springer, Berlin, Heidelberg, 1984, p. 1-59.
13. Z. Foued, B. Said, C. Esperanza, B. Fatma-Zohra, B. Djafer, J. Francisco and C. Baltá, *J. Polym. Eng*. **2014**, *34*, 431–439.
14. F. Romani, R. Corrieri, V. Braga and F. Ciardelli, *Polymer*, **2002**, *43*, 1115–1131.
15. S. Johannes, Ö. Aybike, E. Carsten and B. Udo, *Eur. J. Pharm. Biopharm*, **2010**,*74*, 2-13.
16. B. Said, C. Esperanza, L. Maria, Z. Foued, K. Souhila, T. Habiba, Djafer. B, J. Francisco and C. Baltá. *J. Polym. Eng*., **2012**, *32*, 143–151.
17. Q. Huaili, Z. Shimin, L. Huiju, X. Shaobo, Y. Mingshu and S. Deyan, *Polymer*, **2005**, *46*, 3149-3156.
18. M. Sandrine, M. Bénédicte, G. David and G. Jean-Luc, *Chem. Mater*., **2004**, *16* ,377-383.
19. G. Lu, A. Linsebigler and J. T. Yates, *J. Phys. Chem*., **1995**, *99*, 7626-7631.
20. J. Mungkalasiri, L. Bedel, F. Emieux, J. Doré, F. N. R. Renaud and F. Maury, *Surf Coat Tech*., **2009**, *204*, 887–892.